

## Conductance values of alkanedithiol molecular junctions

M Teresa González, Jan Brunner, Roman Huber, Songmei Wu, Christian Schönenberger and Michel Calame<sup>1</sup>

Departement für Physik, Universität Basel, Klingelbergstrasse 82, CH-4056 Basel, Switzerland

E-mail: [teresa.gonzalez@unibas.ch](mailto:teresa.gonzalez@unibas.ch) and [michel.calame@unibas.ch](mailto:michel.calame@unibas.ch)

*New Journal of Physics* **10** (2008) 065018 (9pp)

Received 27 February 2008

Published 30 June 2008

Online at <http://www.njp.org/>

doi:10.1088/1367-2630/10/6/065018

**Abstract.** We study the electrical conductance of octanedithiol molecular junctions using a mechanically controllable break-junction setup. The stability of the system allows control of whether the electrodes get into contact before each new molecular junction formation or not (contact and non-contact modes). We find three characteristic conductance values for octanedithiol. Well-defined peaks in the conductance histograms at multiples of  $1.2 \times 10^{-5} G_0$  suggest that this value corresponds to the conductance of a single molecular junction conductance. Reproducible features are also observed at  $4.5 \times 10^{-5}$  and  $2.3 \times 10^{-4} G_0$ . The first value has the strongest statistical weight, whereas the second is only observed in the non-contact mode. We propose that these two values reflect the formation of several molecular junctions in parallel between the electrodes.

### Contents

<b>1. Introduction</b>	<b>2</b>
<b>2. Experimental details</b>	<b>2</b>
<b>3. Results and discussion</b>	<b>4</b>
<b>4. Conclusion</b>	<b>8</b>
<b>Acknowledgments</b>	<b>8</b>
<b>References</b>	<b>8</b>

<sup>1</sup> Author to whom any correspondence should be addressed.

## 1. Introduction

Alkanes, simple saturated chains of carbon atoms, have been the most popular test-molecules for studies of the electrical conductance of molecular junctions in the last few years [1]–[8]. Their chemical stability and large highest occupied molecular orbital (HOMO)–lowest unoccupied molecular orbital (LUMO) gap (of several electron volts) make them ideal for investigating the contribution of the molecule–electrode coupling to the total junction conductance [9]. They have been, for example, used as a platform for testing the anchoring efficiency of different chemical groups [10]–[12]. It has also been suggested that different atomic arrangements at the molecule–electrode bond can produce a variation by more than one order of magnitude in the conductance of alkane-based molecular junctions [4, 6, 8, 13].

A molecular junction here is defined as the device formed by a single molecule chemically bound to two gold electrodes. The electrical properties of such junctions are most successfully investigated by break-junction techniques based on scanning tunneling microscope (STM) arrangements [1, 3], or on mechanically controllable break junctions (MCBJ) [14, 15]. The reliability of these techniques has been well established as shown by the good agreement found between results from different laboratories [4, 5, 7, 16].

Recently, several groups have reported that molecular junctions based on alkanedithiols are typically characterized by three conductance values. These can be labeled  $G^l$  (low),  $G^m$  (medium) and  $G^h$  (high). The authors explain that each  $G$  value corresponds to a single molecular junction of a different type, characterized by the atomic configuration at the molecule–electrode bond [4, 6, 8, 13]. Changes in the internal alkane conformation (from *trans* to *gauche*) can also result in a significantly different conductance value [6, 8, 13]. These assumptions are supported by several *ab initio* calculations that predict a significant conductance variation upon atomic rearrangement [8], [17]–[19].

There is good agreement among the values assigned to  $G^l$ ,  $G^m$  and  $G^h$  by different groups [4, 6, 8, 13]. Also, individual  $G$  values reported in initial experiments (where only a restricted conductance range was explored) [1, 3] are in good agreement with one of the three conductance values. The important exception is  $G^h$ . While this value is reported by several groups working with STM break junctions [1, 8, 13], no molecular signature was observed in that conductance range in MCBJ experiments [5].

In this work, we explore the corresponding three conductance regimes for octanedithiol molecular junctions using an MCBJ setup. We have performed the experiments in two ways: in the first approach (contact mode), our gold electrodes are brought into contact before each new molecular junction formation. In the second (non-contact mode), the electrodes are only closely approached but without touching each other. Surprisingly, we have observed a significant signal at  $G^h$  only in non-contact mode. We see *a priori* no reason why certain atomic configurations at the bonds should be forbidden in contact mode. We therefore suggest an alternative explanation: the signature at  $G^h$  reflects the formation of a larger number of molecular junctions in parallel between the electrodes.

## 2. Experimental details

Details on the preparation of the break-junction samples and the experimental setup have been described elsewhere [5, 20]. Briefly, electrically isolated stainless-steel sheets are used as substrates (see figure 1(a)). Gold leads are realized by electron-beam lithography, followed by

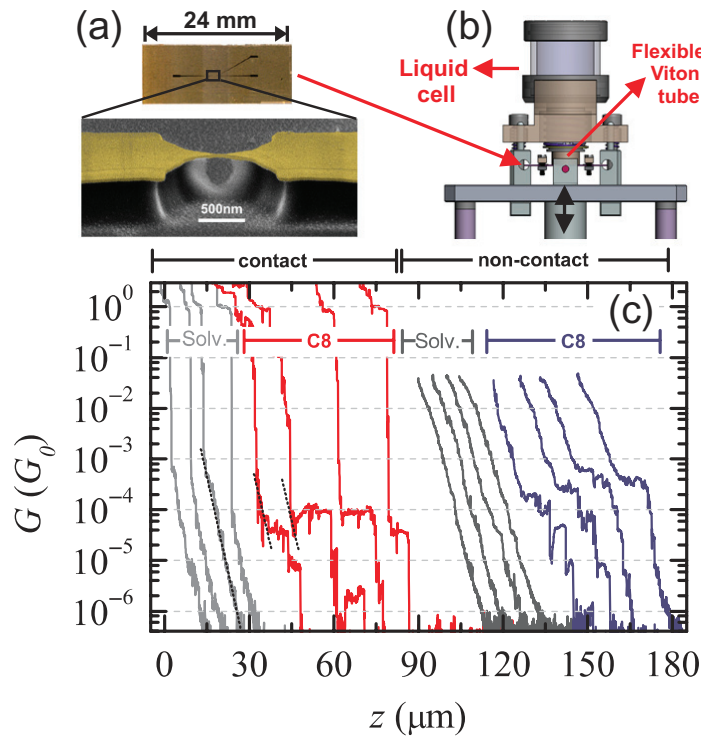


**Figure 1.** (a) Break-junction samples: stainless-steel substrate covered by an insulating polyimide. The SEM picture shows the free-standing bridge on the gold lead patterned by electron-beam lithography. (b) Schematics of our MCBJ set-up equipped with a liquid cell. (c) Individual  $G(z)$  traces in contact and non-contact. In both cases, the curves obtained when C8 is in solution present well-defined plateaus, whereas a simple tunneling exponential decay is observed in pure solvent. Note that, for the non-contact mode, new plateaus develop between  $10^{-4}$  and  $10^{-3} G_0$ .

gold evaporation. By oxygen plasma etching, a free-standing bridge is defined in the narrowest middle region of the gold wire, as shown in the SEM picture of figure 1(a).

Figure 1(b) schematizes our bending mechanism. The sample is bent and relaxed when the pushing rod at the bottom is moved up and down, respectively. When bending, the pulling stress at the free-standing bridge concentrates in the narrow, middle region that eventually breaks. Then, the size of the opened gap,  $\Delta d$ , keeps a linear relationship with the vertical motion of the rod,  $\Delta z$ . The attenuation factor is [20]  $a = \Delta d / \Delta z = 1.6 - 4 \times 10^{-5}$ . A liquid cell, which is terminated in a flexible Viton tube, is placed over the substrate, covering the free-standing gold bridge. All the experiments were performed at room temperature in mesitylene.

During the bending and relaxing of the substrates (opening and closing of the gold junction), the variation of the total conductance  $G(z)$  (with  $z$  being the vertical position of the pushing-rod) is monitored at a constant bias voltage of 0.2 V. A home-built current-voltage amplifier, which automatically adjusts its gain between  $10 \text{ V mA}^{-1}$  and  $1 \text{ V nA}^{-1}$ , guarantees that the junction conductance is registered from more than  $50 G_0$  ( $G_0 = 2e^2 h^{-1}$ ), down to  $5 \times 10^{-7} G_0$ .

To determine the molecular junction conductance, a statistical study is performed. We have measured several collections of 100 consecutive  $G(z)$  curves, and built conductance

histograms as explained in [5]. The initial and final positions of each curve are defined by conductance values: during the opening,  $z$  is increased until  $G$  decreases below a certain low threshold value,  $G_{\text{th}}^{\text{lo}}$ . We set this value slightly above our detection limit<sup>1</sup>. Accordingly, during closing,  $z$  is decreased until  $G$  reaches a high threshold  $G_{\text{th}}^{\text{hi}}$ . This value determines how much the gold electrodes approach each other. In this work, two values of  $G_{\text{th}}^{\text{hi}}$  were explored. The first one,  $G_{\text{th}}^{\text{hi}} = 50 G_0$ , is above  $G_0$  and guarantees that the electrodes will contact before each new opening. We call this regime ‘contact mode’. For the second one,  $G_{\text{th}}^{\text{hi}} \approx 10^{-2} - 10^{-1} G_0$ , the electrodes do not approach enough to touch each other. We call this regime ‘non-contact mode’.

### 3. Results and discussion

Figure 1(c) shows typical  $G(z)$  curves measured during opening (increasing  $z$ ), both when the gold junctions are immersed in pure solvent (mesitylene), and in a 1 mM solution of octanedithiol (C8). In contact mode (left part of figure 1(c)), the breaking of the last one-gold-atom contact is easily identified in each curve by a plateau at  $1 G_0$ , followed by a sudden  $G$  decay of around three orders of magnitude [5]. This decay corresponds to a rapid gap opening, corresponding to the size of 1–2 gold atoms. In pure solvent,  $G$  then simply decays exponentially with  $z$ , as is characteristic of electrode-to-electrode tunneling. This tells us that the gap size grows linearly with  $z$ , and, thus, the atomic arrangement at the electrodes’ apex does not change further within the time of the experiment. In the non-contact mode (figure 1(c), right), there is no abrupt  $G$  decay as the gap remains open during the whole measurement. In both contact and non-contact modes, the presence of C8 molecules translates into the appearance of plateaus several orders of magnitude below  $1 G_0$  (in 60–90% of the curves).

In figure 1(c), we see that plateaus in the range  $10^{-3} - 10^{-4} G_0$  only appear in the non-contact mode. The difference between the two modes appears more clearly when conductance histograms are built from the  $G(z)$  curves. Figure 2(a) compares the log  $G$ -histograms obtained from collections of 100  $G(z)$  curves such as those of figure 1(c). They were built calculating the logarithm of  $G$  for all the measured  $G(z)$  curves. The constant bin size is  $\Delta \log(G/G_0) = 0.03$  (we stress here that our auto-range  $IV$ -converter amplifier is linear). This representation shows the whole overview of the measured  $G$ -range, and ensures that we do not miss any signal characteristic of the molecular junctions.

Focusing first on the contact mode (gray and red histograms, figure 2(a)), below the well-defined peak at  $1 G_0$  (one-gold-atom bridge), we only see the nearly flat contribution of gold-to-gold tunneling in pure solvent<sup>2</sup>. In contrast, a pronounced peak develops between  $-5$  and  $-3.5$  when C8 is present (red histogram). As shown in [21], a Gaussian curve can be fitted to the global peak, from which the characteristic molecular conductance can be simply extracted. This Gaussian is depicted by a dashed line in figure 2(a). The corresponding linear  $G$ -histogram in that conductance range can also be seen in figure 2(b) (constant bin size in linear scale:  $\Delta G = 4 \times 10^{-6} G_0$ ). After the tunneling background subtraction [5], the Gaussian curve results in a skewed curve that describes very well the overall shape of the histogram, both presenting a maximum at the same position. The mean  $G$ -value at the maximum, obtained from eight sets of 100 curves in three different samples, is  $G_A = 4.5 \pm 1.1 \times 10^{-5} G_0$ . This corresponds to the

<sup>1</sup> The pushing-rod moves up an additional fixed distance of  $100 \mu\text{m}$  once  $G_{\text{th}}^{\text{lo}}$  is reached.

<sup>2</sup> Deviation from the horizontal can occur because, after the  $1 G_0$  plateau, the  $G$  value from which the tunneling behavior starts varies in each curve, typically, between  $10^{-2}$  and  $10^{-5} G_0$ , see figure 1(c).

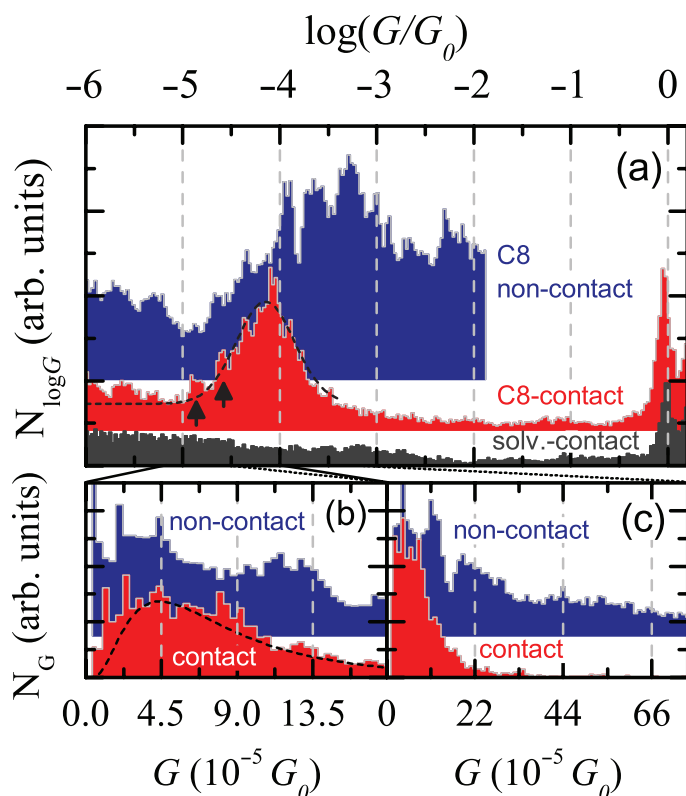


**Figure 2.** (a) Log  $G$ -histograms built from sets of 100  $G(z)$  traces (figure 1(c)). A peak structure is observed when C8 is in solution in contrast to the flat, pure solvent histogram. The broad peak in contact mode can be fitted to a Gaussian curve (dotted line). A finer, superimposed structure is observed (black arrows). In the non-contact mode, new peaks appear between  $-4$  and  $-3$ . (b) and (c) Linear  $G$ -histograms for C8 in two different  $G$  ranges. A peak centered at  $2.2 \times 10^{-4} G_0$  appears only in the non-contact mode.

most probable conductance of the molecular junction, and agrees with the value reported by several groups for C8 [4, 5, 7].

If we move now to the non-contact mode (blue histogram), we see that new peaks appear between  $-4$  and  $-3$  in the log  $G$ -histogram of figure 2(a). The linear histograms for both modes in that conductance regime (bin size:  $\Delta G = 1 \times 10^{-5} G_0$ ) are compared in figure 2(c). A well-defined peak appears at  $2.2 \times 10^{-4} G_0$  only in the non-contact mode. Averaging over three different samples, the mean  $G$ -value for this new peak is  $G_B = 2.3 \pm 0.3 \times 10^{-4} G_0$ . This value is very close to  $2.5 \times 10^{-4} G_0$ , the first conductance value reported for C8 by Xu and Tao [1], or  $2.7 \times 10^{-4} G_0$  observed by Li *et al* [8].

In [4, 8, 13], histograms with several families of peaks are reported for alkanedithiols. A family is defined by a group of peaks centered at  $G$ -values given by  $nG^1$ , where  $n$  is an integer number and  $G^1$  is the principal conductance (the conductance at the first peak of the family). Following the idea introduced by Cui *et al* [2],  $G^1$  is considered the conductance of a single molecular junction, and the whole peak family accounts for the junctions formed by  $n$  identical molecular junctions in parallel. Grouping the peaks in different families means that several  $G^1$  are possible. It is interpreted that the details of the molecule–electrode

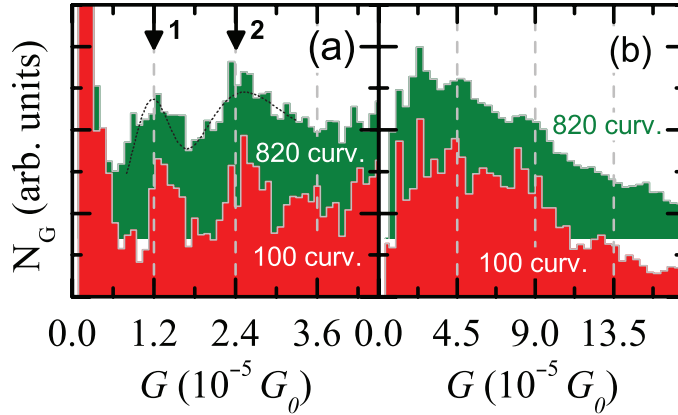


**Figure 3.** Linear histograms in two different conductance regimes obtained in the contact mode. The upper histograms are built from eight sets of approximately 100  $G(z)$  curves recorded on three different samples. In these histograms, peaks at multiples of  $G_C = 1.2 \times 10^{-5} G_0$  are still easy to distinguish (a), whereas the profile of the overall peak becomes smoother (b).

bond define different molecular junctions realizations with significantly different  $G^1$  values [4, 6, 8, 13]. For C8, up to three  $G^1$  are distinguished [4, 8]:  $G^1 \simeq 1 \times 10^{-5} G_0$ ,  $G^m \simeq 5 \times 10^{-5} G_0$  and  $G^h \simeq 2.5 \times 10^{-4} G_0$ .

The conductance values  $G_A$  (contact and non-contact modes) and  $G_B$  (only non-contact mode) reported here are in excellent agreement with  $G^m$  and  $G^h$ . However, the fact that junctions with conductance  $G_B$  are only formed in the non-contact mode does not support the idea that  $G_A$  and  $G_B$  correspond to two different molecular junction realizations. In the contact mode, new electrode apexes will be formed after the electrodes are brought into contact. We see no reason why certain atomic conformations at the apexes should be forbidden especially in this mode. Also, even when the peaks corresponding to  $nG_A$  and  $nG_B$  are reported for  $n$  up to 3, [4, 8], there is no significant contribution of signal at for instance  $G_A + G_B$  or  $G_A + 2G_B$  in the reported data, which should be expected as well.

In figure 2(b), in the contact mode, apart from the overall shape described by the fitted curve, it can be argued that individual peaks centered at multiple values of  $G_A$  can be differentiated. However, these peaks are not well defined and the multiplicity at  $n = 1, 2$  and  $3$  is not obvious in our data<sup>3</sup>. Other studies in the literature show similar qualitative results, with only one skewed peak distinguishable in the histograms [7, 11, 12]. Note that, in the non-contact mode, there is also a new peak appearing at around  $1.1\text{--}1.2 \times 10^{-4} G_0$ , which could be interpreted as a  $2G_A$  peak, although its position is intermediate between 2 and 3  $G_A$ .

A superposed finer structure can nevertheless be recognized in the histograms of figure 2. This is clearer in contact mode where smaller peaks in the log-histogram of figure 2(a) are easy to distinguish (black arrows). In linear scale, an additional histogram focusing on this regime is needed. Figure 3(a) shows such a histogram (bin size:  $\Delta G = 9 \times 10^{-7} G_0$ ). Well-defined individual peaks at multiples of  $G_C = 1.2 \times 10^{-5} G_0$  are evident here. This value agrees very well with the conductance reported for C8 by Haiss *et al* [3] ( $1.3 \pm 0.1 \times 10^{-5} G_0$ ), and the  $G^1$  reported by Li *et al* [8] ( $1.1 \pm 0.1 \times 10^{-5} G_0$ ).

<sup>3</sup> No curve selection has been performed in our histograms. We have also verified that, as explained in [5], selecting manually only the  $G(z)$  points contained in the plateaus does not change the profile of our histograms.

In order to establish to what extent these results depend on limited statistics (100 curves), we have considered several 100-curve batches from three different samples. Figure 3 shows the histograms built from up to 820 conductance traces. The peaks at  $G_C$  and  $2G_C$  are now broader than in the 100-curve histogram, while no clear peak appears at  $3G_C$ , reflecting a larger dispersion in the plateau conductance values as the number of measured curves is increased. Nevertheless, the first two peaks can still be independently distinguished. The shape of the overall peak shown in figure 3(b) also persists, but the profile of the histogram becomes smoother. Note that there are only slight protrusions at  $G_A = 4.5 \times 10^{-5} G_0$  and  $2G_A$ , without clear peaks developing at these positions.

These results lead us to propose the following explanation for the observed peaks in the histograms. We only observed robust individual peaks (that is: peak structures remaining clearly visible when increasing the statistics of the histogram) at  $nG_C$  ( $n = 1$  and  $2$ ). We therefore consider  $G_C$  to be the best candidate for the conductance of a molecular junction when a single molecule governs transport. We interpret that higher characteristic  $G$ -values reflect the formation of molecular junctions with several molecules bound in parallel between the electrodes. By a simple Gaussian fit to the first peaks in figure 3(a) (dotted line), we can estimate the width of the first peak as  $w_1 = 5.6 \times 10^{-6} G_0$ . This is roughly 50% of  $G_C$ . If all the peaks are then due to  $n$  independent molecular junctions with a 50% variation in conductance, the  $n$ th peak will appear at  $G_n = nG_C$ , and have a width  $w_n = \sqrt{n} w_1$ . The relative width  $w_n/G_n = \sqrt{n} w_1/G_C$  becomes 100% already for the fourth peak. We can therefore expect to see only distinct peaks up to  $n = 2$  or  $3$ , while a broader signal will account for larger  $n$  values. This is indeed what we see in our experiments.

Notice here that, even when the weight of the peaks at  $G_C$  and  $2G_C$  in the overall histograms is small, this does not mean that they are produced by only a few plateaus in the curves. About 50–60% of the curves showing plateaus have some of them appearing in the interval  $0.8$ – $3 \times 10^{-5} G_0$ . These plateaus appear, however, often after plateaus at higher conductance and are comparatively shorter. In the picture of many molecules bridging the electrodes in parallel, the conductance of one or two molecules will only be observable when all the others have detached. A lower weight in the histograms can then be expected.

Considering the geometry of our experiment, there is *a priori* no reason for limiting the formation of molecular junctions to 2 or 3 molecules in parallel. On the contrary, the continuous  $G$ -decay of individual curves (without jumps from lower to higher conductance, which would signal a junction formation) suggests that one or several molecular junctions can be formed between the electrodes even before the last gold atoms are split at the very tip. The large size of the electrodes in comparison with the molecules leads us to expect a larger number of molecular junctions as the most probable situation. It is consistent as well to expect the formation of a larger number of molecular junctions in parallel in the non-contact mode, as the Au relaxation at the electrode apexes will favor blunt tips and larger electrode areas.

The maxima around  $G_A$  and  $G_B$  seem to indicate that specific numbers of molecular junctions in parallel can be especially favorable. It is well known that nanometric gold structures tend to have preferred sizes. Colloids with 13, 55 or 309 atoms (1, 2 and 4 full shells) are most favorably formed in the proper conditions (see e.g. [22]). Also shell effects have been observed to give preferred widths to nanowires formed by MCBJ [23, 24]. It is therefore not surprising that the apexes of our electrodes, which are broken in a thiol solution, tend to have preferred sizes that are reproducible in various experiments. In fact, although the conductance values  $G_A$  and  $G_B$  do not seem to correspond to single molecular junctions, they are well reproduced in different break-junction experiments and constitute as good molecular fingerprints as  $G_C$  is.

Finally, we note that a significant number of curves (around 30%) present plateaus in the range  $1-5 \times 10^{-6} G_0$ . In figure 2(a), a peak structure can be seen in this range. However, the  $G$ -values of these plateaus are more dispersed, and the peaks are washed out when averaging many  $G(z)$  traces.

A recent work of Xu [25] reports  $G_B$  as the dominant value observed using STM break junctions. However, a value ten times smaller (close to  $G_C$ ) is also clearly observed when a sinusoidal modulation is superimposed to the motion of the tip with respect to the substrate. We think that these results are compatible with our assumption, as the oscillating motion could favor the formation of only a small number of molecular junctions even when the apexes of the electrodes present a larger area. Independently, Jang *et al* [7] built histograms of only the last conductance step of their  $G(z)$  curves. They observed no signal at  $G_B$ , which also suggests that  $G_B$  does not correspond to a single molecular junction conductance.

#### 4. Conclusion

In summary, we have shown that MCBJ permit fine enough control of the electrodes' motion to allow choosing between two modes during the experiments (contact and non-contact). Using octanedithiol as test molecule, we have found three characteristic conductance values  $G_C = 1.2 \times 10^{-5} G_0$  ( $\simeq G^l$ ),  $G_A = 4.5 \times 10^{-5} G_0$  ( $\simeq G^m$ ), and  $G_B = 2.3 \times 10^{-4} G_0$  ( $\simeq G^h$ ). Individual peaks at  $nG_C$ , with  $n = 1$  and 2 are clearly observed, whereas no clear multiplicity is observed in our data for  $G_A$  and  $G_B$ . We suggest that only  $G_C$  can be interpreted as the conductance of a single molecular junction. A reproducible feature with strong statistical weight is also observed at  $G_A$ , which in our view reflects a most favorable microscopic arrangement with more than one, but only few, molecular junctions formed in parallel.  $G_B$  is only favored in the non-contact mode, when the area at the electrodes' apexes becomes larger and can accommodate an even larger number of molecular junctions in parallel.

#### Acknowledgments

We thank M Steinacher and H Breitenstein for their technical support, and M Mayor's group for fruitful discussions. This work was supported by the Swiss National Center of Competence in Research 'Nanoscale Science', the Swiss National Science Foundation, and the European Science Foundation through the Eurocore program on Self-Organized Nanostructures (SONS). TG acknowledges the 'Ministerio de Educación y Ciencia' and the 'Freie Akademische Gesellschaft' (FAG), for financial support.

#### References

- [1] Xu B and Tao N J 2003 *Science* **301** 1221–3
- [2] Cui X D, Primak A, Zarate X, Tomfohr J, Sankey O F, Moore A L, Moore T A, Gust D, Harris G and Lindsay S M 2001 *Science* **294** 571–4
- [3] Haiss W, Nichols R J, van Zalinge H, Higgins S J, Bethell D and Schiffrin D J 2004 *Phys. Chem. Chem. Phys.* **6** 4330–7
- [4] Li X, He J, Hihath J, Xu B, Lindsay S M and Tao N 2006 *J. Am. Chem. Soc.* **128** 2135–41
- [5] González M T, Wu S, Huber R, van der Molen S J, Schönenberger C and Calame M 2006 *Nano Lett.* **6** 2238–42

- [6] Fujihira M, Suzuki M, Fujii S and Nishikawa A 2006 *Phys. Chem. Chem. Phys.* **8** 3876–84
- [7] Jang S-Y, Reddy P, Majumdar A and Segalman R A 2006 *Nano Lett.* **6** 2362–7
- [8] Li C, Pobelov I, Wandlowski T, Bagrets A, Arnold A and Evers F 2008 *J. Am. Chem. Soc.* **130** 318–26
- [9] Akkerman H B and de Boer B 2008 *J. Phys.: Condens. Matter* **20** 013001
- [10] Chen F, Li X, Hihath J, Huang Z and Tao N 2006 *J. Am. Chem. Soc.* **128** 15874–81
- [11] Venkataraman L, Klare J E, Tam I W, Nuckolls C, Hybertsen M S and Steigerwald M L 2006 *Nano Lett.* **6** 458–62
- [12] Park Y S, Whalley A C, Kamenetska M, Steigerwald M L, Hybertsen M S, Nuckolls C and Venkataraman L 2007 *J. Am. Chem. Soc.* **129** 15768–9
- [13] Nishikawa A, Tobita J, Kato Y, Fujii S, Suzuki M and Fujihira M 2007 *Nanotechnology* **18** 424005
- [14] Reed M A, Zhou C, Muller C J, Burgin T P and Tour J M 1997 *Science* **278** 252–4
- [15] Reichert J, Ochs R, Beckmann D, Weber H B, Mayor M and Löhneysen H 2002 *Phys. Rev. Lett.* **88** 176804
- [16] Li Z, Pobelov I, Han B, Wandlowski T, Blaszczyk A and Mayor M 2007 *Nanotechnology* **18** 044018
- [17] Lee M, Speyer G and Sankey O F 2006 *Phys. Status Solidi b* **243** 2021–9
- [18] Müller K-H 2006 *Phys. Rev. B* **73** 045403
- [19] Krag C 2007 *Master's Thesis* Department of Micro and Nanotechnology, Technical University of Denmark
- [20] Grüter L, González M T, Huber R, Calame M and Schönenberger C 2005 *Small* **1** 1067–70
- [21] Huber R *et al* 2008 *J. Am. Chem. Soc.* **130** 1080–4
- [22] Schmid G 2001 *Nanoscale Materials in Chemistry* ed K Klabunde (New York: Wiley) chapter 2 p 15
- [23] Agraït N, Yeyati A L and van Ruitenbeek J M 2003 *Phys. Rep.* **377** 81–279
- [24] Kondo Y and Takayanagi K 2000 *Science* **289** 606–8
- [25] Xu B 2007 *Small* **3** 2061–4